D.L. Cooper (Editor)
Valence Bond Theory
Theoretical and Computational Chemistry, Vol. 10

Chapter 3

Complete active space valence bond (CASVB) method and its application to chemical reactions

Haruyuki Nakano, Kazushi Sorakubo, Kenichi Nakayama, and Kimihiko Hirao

Department of Applied Chemistry, Graduate School of Engineering, University of Tokyo, 7-3-1 Hongo, Bunkyo-ku, Tokyo 113-8656, Japan

The complete active space valence bond (CASVB) method is an approach for interpreting complete active space self-consistent field (CASSCF) wave functions by means of valence bond resonance structures built on atom-like localized orbitals. The transformation from CASSCF to CASVB wave functions does not change the variational space, and thus it is done without loss of information on the total energy and wave function. In the present article, some applications of the CASVB method to chemical reactions are reviewed following a brief introduction to this method: unimolecular dissociation reaction of formaldehyde, $H_2CO \rightarrow H_2+CO$, and hydrogen exchange reactions, $H_2+X \rightarrow H+HX$ (X=F, Cl, Br, and I).

1. INTRODUCTION

The complete active space self-consistent field (CASSCF) method is one of the electronic structure theories that is employed most frequently in the study of chemical reactions. This method is feasible and gives potential energy surfaces of good quality, and hence it is also used as a starting point for higher-level multireference methods. In fact, the CASSCF method has many advantages: (1) it is well defined on the whole potential energy surface of a chemical reaction if an appropriate active space is chosen; (2) it is applicable to excited states as well as the ground state in a single framework, and (3) it provides size-consistent results, etc. However, it often generates too many configurations, and therefore there is a problem as to how we could extract a chemical description from the lengthy CASSCF wave functions.

The complete active space valence bond (CASVB) method [1,2] is a solution to this problem. Classical valence bond (VB) theory is very successful in providing a qualitative explanation for many aspects. Chemists are familiar with the localized molecular orbitals (LMO) and the classical VB resonance concepts.

If modern accurate wave functions such as CASSCF can be represented in terms of such well-known concepts, chemists' intuition and experiences will give a firm theoretical basis and the role of computational chemistry will undoubtedly expand.

The CASVB functions can be obtained by transforming the canonical CASSCF functions without loss of energy. First we transform the CASSCF delocalized MO to localized MO using the arbitrariness in the definition of the active orbitals. Then we perform the full configuration interaction (CI) calculation again in the active space. Here, we also use the arbitrariness in the definition of the expansion configuration functions. The configuration functions used are spin-paired functions based on the LMOs. This form of spin eigenfunctions plays a special role in the VB method. The CASVB wave functions can be readily interpreted in terms of the well-known classical VB resonance structures. The total CASVB wave function is identical to the canonical CASSCF wave function. In other words, the MO description and the VB description are equivalent, at least at the level of CASSCF. The CASVB method provides an alternative tool for describing the correlated wave functions.

With this method, we clarified the electronic structures of the ground and excited states of benzene, butadiene, methane, and hydrogen molecules [1,2]. We also applied the method to valence excited states of polyenes [3] and their cations [4]. In previous studies, we put our focus on the formalism of CASVB and its applicability to molecules in their equilibrium structures.

Even today, however, it is not a simple task to obtain chemical pictures at the transition state (TS) or along a reaction path. Discussion on the nature of TS is, for instance, often conducted using other features such as molecular structures and energy profiles rather than the wave functions themselves: if the bond length at TS is closer to that of the product than reactant, it is called a *late* TS, or if the reaction is highly exothermic, this reaction is assumed to proceed via an *early* TS. These discussions are qualitative and ambiguous. A more quantitative and clear-cut chemical description is necessary.

In this article, we present applications of CASVB to chemical reactions: the unimolecular dissociation reaction of formaldehyde, $H_2CO \rightarrow H_2+CO$ [5], and a series of hydrogen exchange reactions, $H_2+X \rightarrow H+HX$ (X=F, Cl, Br, and I). The method in this article is based on the occupation numbers of VB structures that are defined by the weights of the spin-paired functions in the CASVB functions, so that we could obtain a quantitative description of the nature of electronic structures and chemical bonds even during reactions.

In Sec. 2, we briefly survey the CASVB method. In Sec. 3, the CASVB method is applied to the unimolecular dissociation $H_2CO \rightarrow H_2+CO$ and the hydrogen exchange reactions $H_2+X \rightarrow H+HX$ (X=F, Cl, Br, and I), and the applicability to the reaction is discussed. Conclusions are given in Sec. 4.

2. OVERVIEW OF CASVB METHOD

We have proposed two types of CASVB method. The first one is a method where the valence bond structures are constructed from *orthogonal* localized molecular orbitals (LMOs) [1], and the second is one from *nonorthogonal* localized molecular orbitals [2].

The idea of CASVB is based on the fact that the densities of variational wave functions are invariant under the transformations which hold the variational space unchanged. In the CASSCF case, a complete active space (CAS) is invariant under the linear transformation of active orbitals and also that of configuration state functions (CSFs).

We may re-define the active orbitals utilizing the invariance of the active orbital space. In the CASVB with *nonorthogonal* LMOs, we employ Ruedenberg's procedure of projected localized MOs [6-8] and obtain quasi-atomic CASSCF MOs that have maximal overlaps with atomic orbitals (AOs) of the free atoms. Consider an AO, χ_A, centered on a nucleus A. Diagonalizing the matrix,

$$P_{ij} = \langle \psi_i | \chi_A \rangle \langle \chi_A | \psi_j \rangle \tag{1}$$

in the CASSCF MO basis, ψ_μ, and choosing the eigenvector with the largest eigenvalue gives the LMO, φ_A, which has the maximum overlap with χ_A. Similarly, we can define φ_B, φ_C, ... The LMOs, φ_μ, determined in this manner are nonorthogonal to each other. These atom-adapted LMOs are Ruedenberg orthogonalized, but we leave them as nonorthogonal. On the other hand, in the CASVB with *orthogonal* LMOs, we use LMOs produced by a Boys' localization procedure as $\{\varphi_i\}$ [9].

The full configuration space that is spanned by all possible configurations generated from these quasi-atomic CASSCF MOs is identical to that of full CI space that is constructed from the canonical CASSCF MOs. Thus, we use $\{\varphi_\mu\}$ as orbitals from which a CASVB wave function is constructed. To obtain the corresponding VB structures, we project a canonical CASSCF wave function onto a VB wave function. The projection does not modify the original wave function but simply re-expresses it in the VB language. Let Ψ^{CASSCF} be a CASSCF wave function,

$$\Psi^{\mathrm{CASSCF}} = \sum_i C_i \Phi_i^{\mathrm{CSF}}, \quad \Phi_i^{\mathrm{CSF}} \equiv \Phi_i^{\mathrm{CSF}}\left(\{\psi_i\}\right) \tag{2}$$

where Φ_i^{CSF} are the configuration state functions constructed by the orthogonal orbitals set $\{\psi_i\}$ and C_i are the known CAS-CI expansion coefficients. Simi-

larly define the CASVB function in terms of spin-paired functions as

$$\Psi^{\mathrm{CASVB}} = \sum_{\mathrm{i}} A_i \Phi_i^{\mathrm{VB}} , \quad \Phi_i^{\mathrm{VB}} \equiv \Phi_i^{\mathrm{VB}} \left(\{\varphi_i\} \right) \tag{3}$$

where Φ_i^{VB} are spin-paired functions constructed by LMOs. The number of independent spin-paired functions is equal to the dimension of CAS, and the spaces spanned by $\{\Phi_i^{\mathrm{CSF}}\}$ and $\{\Phi_i^{\mathrm{VB}}\}$ are identical. Since Eqs. (2) and (3) are different expressions of the identical wave function, we may write

$$\sum_j A_j \Phi_j^{\mathrm{VB}} = \sum_j C_j \Phi_j^{\mathrm{CSF}} . \tag{4}$$

Left-multiplying Eqs. (2) and (3) by Φ_i^{CSF} and integrating the products, we get

$$\sum_j \Omega_{ij} A_j = C_i \quad \text{with} \quad \Omega_{ij} = \left\langle \Phi_i^{\mathrm{CSF}} \middle| \Phi_j^{\mathrm{VB}} \right\rangle , \tag{5}$$

whose dimension is equal to the dimension of CAS. Solving this linear equation, we obtain CASVB wave function Ψ^{CASVB}.

The occupation number (or weight) of a VB structure is calculated with

$$n_i = A_i^* \sum_j S_{ij} A_j , \tag{6}$$

where S_{ij} are overlaps between the structures i and j, defined by

$$S_{ij} = \left\langle \Phi_i^{\mathrm{VB}} \middle| \Phi_j^{\mathrm{VB}} \right\rangle , \tag{7}$$

and satisfies the normalization,

$$\sum_i n_i = 1 . \tag{8}$$

Note that the occupation number n_i could be negative because of the nonorthogonality of resonance structures.

Fig. 1 is a schematic expression of coefficient A_i and occupation number n_i in a two dimensional case.

Thorsteinsson et al. also investigated the transformations of CASSCF functions to modern valence bond representations [10-12]. They examined trans-

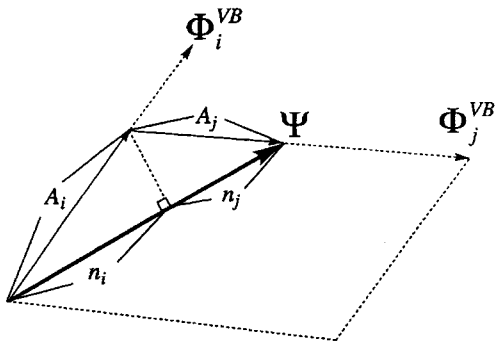

Fig. 1. Schematic expression of coefficient A_i and occupation number n_i in a two dimensional case: $\Psi = A_1\Phi_1^{VB} + A_2\Phi_2^{VB}$.

formations for which the total wave function is dominated by some VB structures (e.g. covalent structures) built from common products of nonorthogonal orbitals. This method was also named "CASVB method." Some recent works of their CASVB method can be seen in review articles [13-15] and references therein.

To obtain more insight into CASVB functions, let us consider the hydrogen molecule as an example [2]. Fig. 2 shows CASSCF, orthogonal localized, nonorthogonal localized, and generalized valence bond (GVB) molecular orbitals obtained for active space CAS(2,2) with correlation consistent valence double zeta (cc-pVDZ) basis set [16] at a bond distance of 0.7 Å. We observe that the orthogonal LMO is deformed significantly from the atomic 1*s* function and has a small tail on the other hydrogen atom due to the orthogonality constraint. The orthogonality requirement between LMOs forces small anti-bonding admixture from orbitals on neighboring atoms into each LMO. On the contrary, the nonorthogonal LMO looks very much like an atomic 1*s* function (the overlap is 0.9859) and the LMOs overlap strongly with each other (0.7775).

The CASSCF wave function for the hydrogen molecule is written as,

$$|\mathrm{CASSCF}\rangle = 0.9948\sigma^2 - 0.1021\sigma^{*2}. \tag{9}$$

This wave function is transformed to CASVB function with orthogonal LMOs,

$$\begin{aligned} |\mathrm{CASVB_{OLMO}}\rangle &= 0.7799\mathscr{A}\left[\varphi_{\mathrm{H_A}}\varphi_{\mathrm{H_B}}(\alpha\beta-\beta\alpha)\right]/\sqrt{2} \\ &\quad + 0.4426\left(\mathscr{A}\left[\varphi_{\mathrm{H_A}}\varphi_{\mathrm{H_A}}\alpha\beta\right]+\mathscr{A}\left[\varphi_{\mathrm{H_B}}\varphi_{\mathrm{H_B}}\alpha\beta\right]\right) \\ &= 0.6082\left[\mathrm{H_A}-\mathrm{H_B}\right]+0.3918\left\{\left[\mathrm{H_A^-}\quad\mathrm{H_B^+}\right]+\left[\mathrm{H_A^+}\quad\mathrm{H_B^-}\right]\right\}, \end{aligned} \tag{10}$$

and with nonorthogonal LMOs,

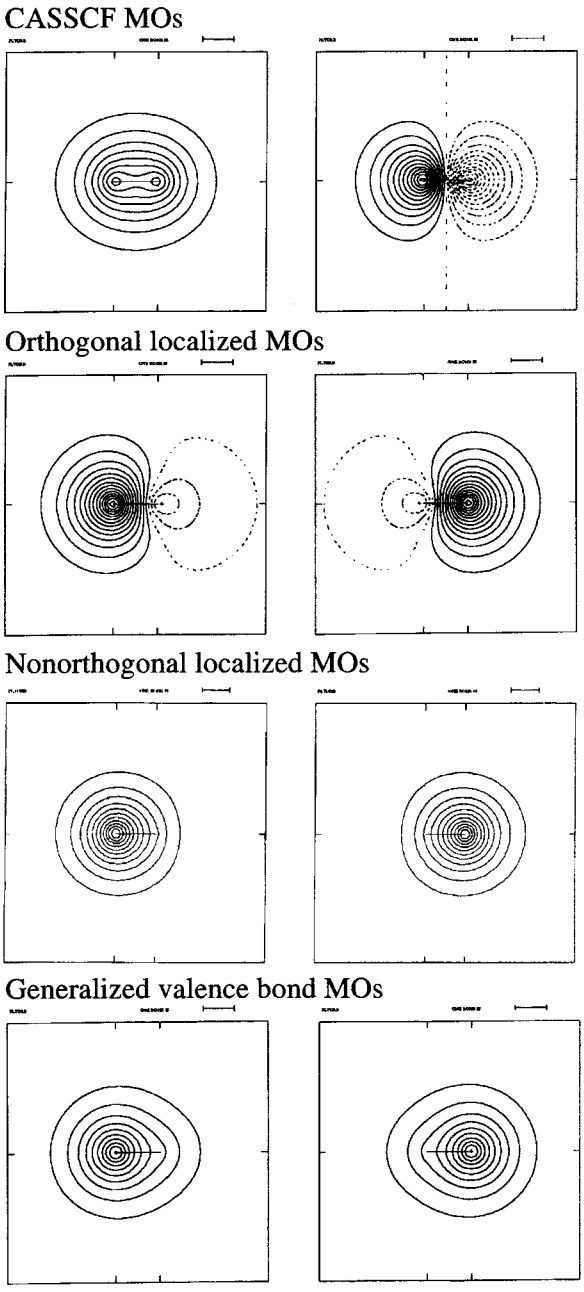

Fig. 2. CASSCF, orthogonal localized, non-orthogonal localized, and generalized valence bond molecular orbitals for the hydrogen molecule.

$$
\begin{aligned}
\left|\mathrm{CASVB_{NLMO}}\right\rangle &= 0.9124\mathscr{A}\left[\varphi_{\mathrm{H_A}}\varphi_{\mathrm{H_B}}(\alpha\beta-\beta\alpha)\right]/\sqrt{2} \\
&\quad +0.0503\left(\mathscr{A}\left[\varphi_{\mathrm{H_A}}\varphi_{\mathrm{H_A}}\alpha\beta\right]+\mathscr{A}\left[\varphi_{\mathrm{H_B}}\varphi_{\mathrm{H_B}}\alpha\beta\right]\right) \\
&= 0.9122\left[\mathrm{H_A}-\mathrm{H_B}\right]+0.0878\left\{\left[\mathrm{H_A^-}\quad \mathrm{H_B^+}\right]+\left[\mathrm{H_A^+}\quad \mathrm{H_B^-}\right]\right\},
\end{aligned}
\tag{11}
$$

where the numbers before the VB structures are occupation numbers n_i (Eq. (6)) and $\mathscr{A}$ denotes the antisymmetrizer. Nonorthogonal LMOs change the

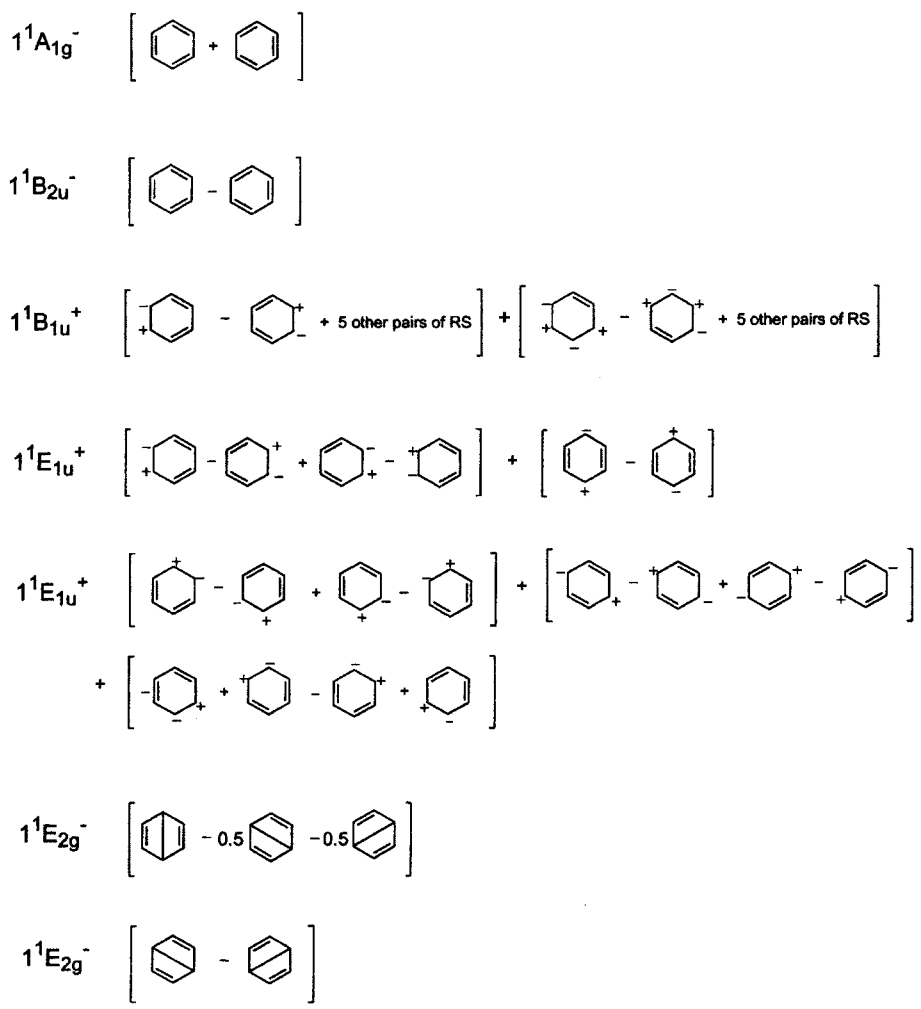

Fig. 3. CASVB description for the ground and $\pi\rightarrow\pi^*$ singlet excited states of benzene.

picture of ionic-covalent resonance dramatically from CASVB with the orthogonal LMOs. Orbital relaxation increases the covalent character of the HH bond and decreases the ionic character. Thus, the nonorthogonal description seems more reasonable conceptually.

The GVB function is also an equivalent expression to the CASSCF and CASVB functions in the CAS(2,2) case. In the GVB description, the wave function is written by the covalent structure only,

$$|\mathrm{GVB}\rangle = \mathscr{A}\left[\varphi_{\mathrm{H_A}}\varphi_{\mathrm{H_B}}(\alpha\beta-\beta\alpha)\right]/\sqrt{2} = \left[\mathrm{H_A}-\mathrm{H_B}\right], \tag{12}$$

and no ionic structure contribution. The orbitals are distorted compared to the nonorthogonal LMOs due to this unphysical constraint.

For one more example, a CASVB description for benzene is given in Fig. 3. See Refs. 1 and 2 for the computational details. The CASVB affords a clear view of the wave functions for the various states. The excitation process is represented in VB theory in terms of the rearrangement of spin couplings and

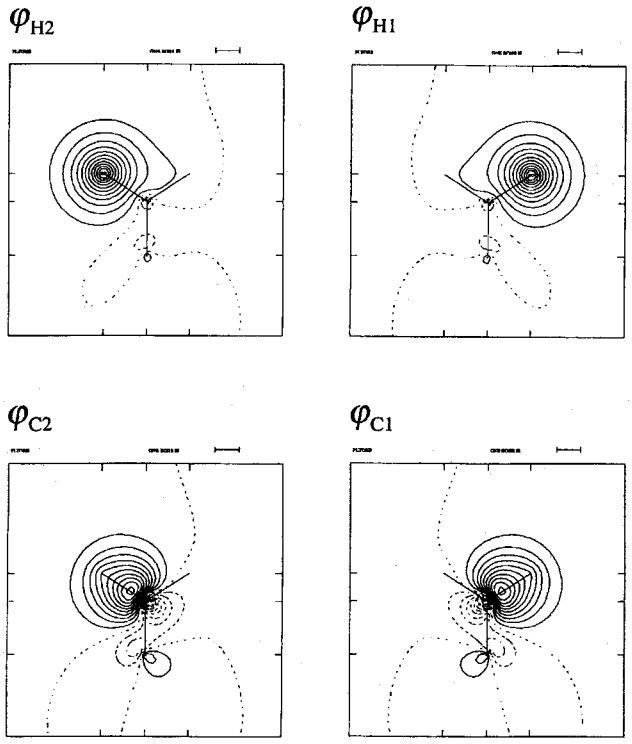

Fig. 4. The nonorthogonal LMOs at the equilibrium structure of H_2CO determined with Ruedenberg's projected localization procedure.

charge transfer. The former generates the covalent excited states and the latter gives rise to the ionic excited states, in which the covalent bond is broken and a new ionic bond is formed. Thus, the singly, doubly, ... , polar structures are generated from their respective *parent* ground state covalent (nonpolar), singly, ... , polar structures.

The ground state is represented by two covalent Kekulé structures as expected. The lowest excited $^1B_{2u}^-$ state is again described by a combination of the Kekulé structure. There are no significant contributions from the Dewar structures or the corresponding orthopolar structures. The linear combinations of the two equivalent Kekulé structures generate the plus and minus states. Their positive combination gives rise to the totally symmetric $^1A_{2g}^-$ ground state, while the negative combination yields the excited $^1B_{2u}^-$ state. The second and third $\pi \rightarrow \pi^*$ excited states are described by a number of ionic structures. There is no contribution from the covalent structures. The ionic character of these states can easily be found from a CASVB description. The highest valence excited states are the covalent $^1E_{2g}^-$ state. The state has a predominantly Dewar character with no contribution from the Kekulé structures. Thus, the Ke-

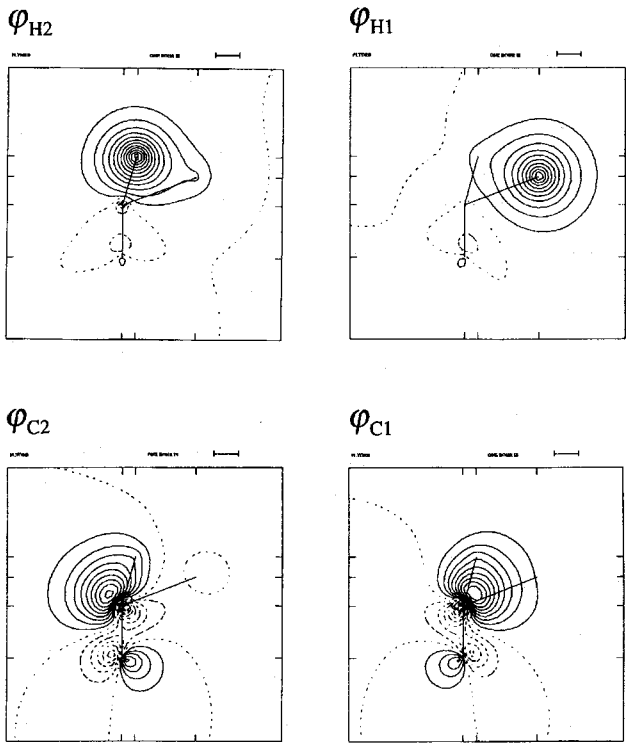

Fig. 5. The nonorthogonal LMOs at the TS structure of the $H_2CO \rightarrow H_2+CO$ reaction.

kulé structures dominate the ground state and the singly excited $1B_{2u}^-$ state while the Dewar structures dominate the doubly excited degenerate $^1E_{2g}^-$ states. The states described by Dewar structures are described by doubly, triply, ... excitations in an MO language.

In this article, we use only the CASVB description with nonorthogonal LMOs. Thus, it is hereafter referred simply as CASVB functions.

3. APPLICATION TO CHEMICAL REACTIONS

In this section, we examine how the electronic structures of molecules during chemical reactions are described by the CASVB method and how they are analyzed with the VB language. Two examples are shown: one is the unimolecular dissociation reaction of formaldehyde, $H_2CO \rightarrow H_2+CO$ [5], and the other is the hydrogen exchange reactions, $H_2+X \rightarrow H+HX$ (X=F, Cl, Br, and I).

Table 1
Spin-paired functions and VB structures of formaldehyde (Normalization and phase factors are omitted.)

Spin-paired function	VB structure	
$\varphi_{H2}\varphi_{C2}(\alpha\beta-\beta\alpha)\cdot\varphi_{C1}\varphi_{H1}(\alpha\beta-\beta\alpha)$	H_2—C—H_1	(I)
$\varphi_{C2}\varphi_{C2}\alpha\beta\cdot\varphi_{C1}\varphi_{H1}(\alpha\beta-\beta\alpha)$ $\varphi_{C1}\varphi_{C1}\alpha\beta\cdot\varphi_{C2}\varphi_{H1}(\alpha\beta-\beta\alpha)$	H_2^+ $^-$C—H_1	(II)
$\varphi_{H2}\varphi_{H2}\alpha\beta\cdot\varphi_{C1}\varphi_{H1}(\alpha\beta-\beta\alpha)$ $\varphi_{H2}\varphi_{H2}\alpha\beta\cdot\varphi_{C2}\varphi_{H1}(\alpha\beta-\beta\alpha)$	H_2^- $^+$C—H_1	(III)
$\varphi_{H2}\varphi_{C2}(\alpha\beta-\beta\alpha)\cdot\varphi_{C1}\varphi_{C1}\alpha\beta$ $\varphi_{H2}\varphi_{C1}(\alpha\beta-\beta\alpha)\cdot\varphi_{C2}\varphi_{C2}\alpha\beta$	H_2—C$^-$ $^+H_1$	(IV)
$\varphi_{H2}\varphi_{C2}(\alpha\beta-\beta\alpha)\cdot\varphi_{H1}\varphi_{H1}\alpha\beta$ $\varphi_{H2}\varphi_{C1}(\alpha\beta-\beta\alpha)\cdot\varphi_{H1}\varphi_{H1}\alpha\beta$	H_2—C$^+$ $^-H_1$	(V)
$\varphi_{C2}\varphi_{C2}\alpha\beta\cdot\varphi_{C1}\varphi_{C1}\alpha\beta$	H_2^+ $^-$C$^-$ $^+H_1$	(VI)
$\varphi_{H2}\varphi_{H2}\alpha\beta\cdot\varphi_{H1}\varphi_{H1}\alpha\beta$	H_2^- $^+$C$^+$ $^-H_1$	(VII)
$\varphi_{H2}\varphi_{H1}(\alpha\beta-\beta\alpha)\cdot\varphi_{C2}\varphi_{C2}\alpha\beta$ $\varphi_{H2}\varphi_{H1}(\alpha\beta-\beta\alpha)\cdot\varphi_{C2}\varphi_{C1}(\alpha\beta-\beta\alpha)$ $\varphi_{H2}\varphi_{H1}(\alpha\beta-\beta\alpha)\cdot\varphi_{C1}\varphi_{C1}\alpha\beta$	H_2 C H_1	(VIII)
$\varphi_{H1}\varphi_{H1}\alpha\beta\cdot\varphi_{C2}\varphi_{C1}(\alpha\beta-\beta\alpha)$	H_2^+ C $^-H_1$	(IX)
$\varphi_{H2}\varphi_{H2}\alpha\beta\cdot\varphi_{C2}\varphi_{C1}(\alpha\beta-\beta\alpha)$	H_2^- C $^+H_1$	(X)
$\varphi_{H2}\varphi_{H2}\alpha\beta\cdot\varphi_{C2}\varphi_{C2}\alpha\beta$ $\varphi_{H2}\varphi_{H2}\alpha\beta\cdot\varphi_{C1}\varphi_{C1}\alpha\beta$ $\varphi_{C2}\varphi_{C2}\alpha\beta\cdot\varphi_{H1}\varphi_{H1}\alpha\beta$ $\varphi_{C1}\varphi_{C1}\alpha\beta\cdot\varphi_{H1}\varphi_{H1}\alpha\beta$	The other (doubly polarized) structures	(XI)

3.1. Unimolecular dissociation reaction of formaldehyde $H_2CO \rightarrow H_2 + CO$

This reaction is Woodward-Hoffmann forbidden and proceeds via a highly asymmetric TS structure. Diabatically H_2CO ($^1A_1$) dissociates to H_2 ($^1\Sigma_g^+$) + CO ($^1\Pi$), while H_2 ($^1\Sigma_g^+$) and CO ($^1\Sigma^+$) interact repulsively and correlate with an excited state of H_2CO. An avoided-crossing of these two diabatic potential energy surfaces gives rise to a barrier for dissociation on the adiabatic ground state potential energy surface.

A qualitatively correct description of the dissociation process requires at least four active electrons in the two CH bonds of H_2CO. During the dissociation process, two electrons, one from each CH bond, pair up to form the HH bond while the other two form a lone pair on C in CO.

The basis set used is Dunning's cc-pVDZ [16]. The CASSCF wave function was obtained with CAS(4,4). The geometries of the equilibrium and TS structures were determined with this basis set and active space. The orbitals were then localized in the active orbital space. The orbitals were transformed so as to have maximum overlap with two carbon sp^2 orbitals and hydrogen $1s$ orbitals. The sp^2 orbitals were used with the fixed hybridization ratio of $2s$ to $2p$ orbitals (1:2) and with a fixed angle of 120° relative to the CO axis

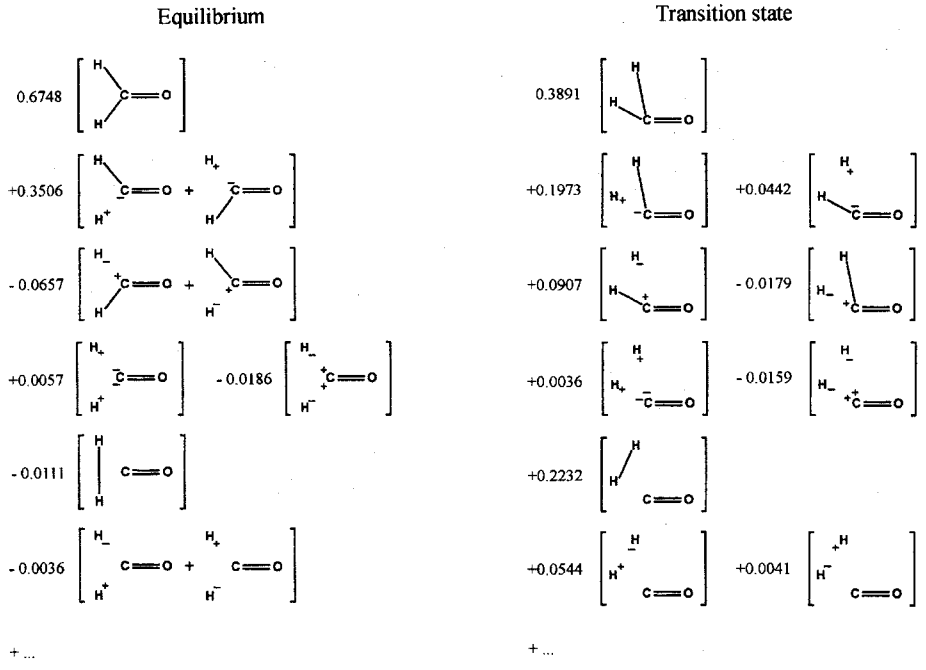

Fig. 6. The CASVB descriptions at the equilibrium and TS structures. The numerical values are occupation numbers.

throughout the reaction. The resulting orbitals are shown in Figs. 4 and 5. All the orbitals are well localized on the atomic centers, except LMOs on the carbon atom, which have a small contribution from the oxygen 2*p* orbital.

There are 20 linearly independent spin-paired functions corresponding to the dimension of CAS(4,4), which are listed in Table 1. Structures (I) to (VII) are classified as CH bond structures and the structures (VIII) to (X) as HH bond structures. Structure (XI) is classified as neither of the above, since these structures can be regarded both as structures polarized further from one of (II) to (V) and (IX) to (X).

The CASVB wave functions obtained for the equilibrium and TS structures are given in Fig. 6.

In the equilibrium structure, the main VB structure is the covalent CH bonds structure (I) as expected. The second most important are those where one of the CH bonds is connected with a covalent bond and the other with an ionic bond made by electron transfer from the hydrogen atom to the carbon atom, (II) and (IV). In contrast, the contribution from the structures that describe electron transfer from the carbon atom to a hydrogen atom is small and negative. The contribution from the HH bond structure (VIII) and ionic structures, (IX) and (X), is very small. The total occupation number of CH bonds is 0.9654, while that of HH bond is −0.0147. This indicates almost no bond formation between two hydrogen atoms in the equilibrium structure.

In the TS structure, the main structure is still the covalent structure (I), although the occupation number decreases. The structure (II), where the longer CH bond is covalent and the shorter CH bond is ionic, is also important, but

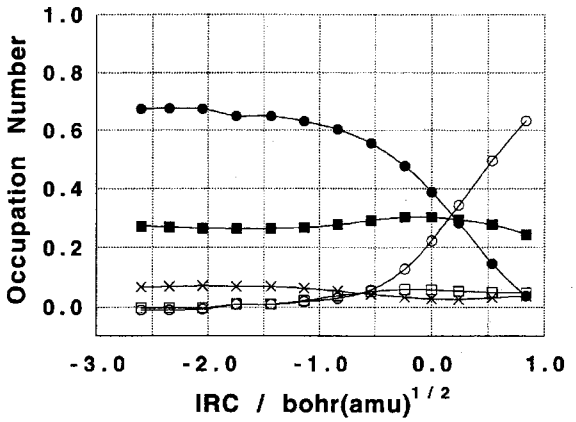

Fig. 7. Changes in the occupation numbers of the covalent CH bonds (●), ionic CH bonds (■), covalent HH bond (○), ionic HH bond (□), and the other (doubly ionic) (×) VB structures of H_2CO along IRC. The origin of the horizontal axis corresponds to the TS and the left end to the equilibrium structure of formaldehyde.

their occupation numbers also decrease. One the other hand, the structure (IV), where the shorter CH bond is covalent and the longer CH bond is ionic, is no longer important. The total occupation number of CH bonds structures is 0.6893, which shows a decrease from the value in the equilibrium structure 0.9654, but it is still large. The total occupation number of HH bond structures is 0.2817. Much of it comes from the covalent contribution (VIII), 0.2232. The contribution from the CH bonds overwhelms the contribution from the HH bond in the TS.

The occupation numbers of the covalent CH bonds, ionic CH bonds, covalent HH bond, ionic HH bond, and the other (doubly ionic) structures are defined by

$$n_{\text{Covalent CH}} = n_{I}, \qquad n_{\text{Ionic CH}} = \sum_{S=II}^{VII} n_{S}, \tag{13}$$

$$n_{\text{Covalent HH}} = n_{VIII}, \qquad n_{\text{Ionic HH}} = n_{IX} + n_{X}, \tag{14}$$

and

$$n_{\text{Doubly Pol.}} = n_{XI}. \tag{15}$$

Using Eqs. (13) and (14), we may further define the total occupation numbers of the CH and HH bond structures,

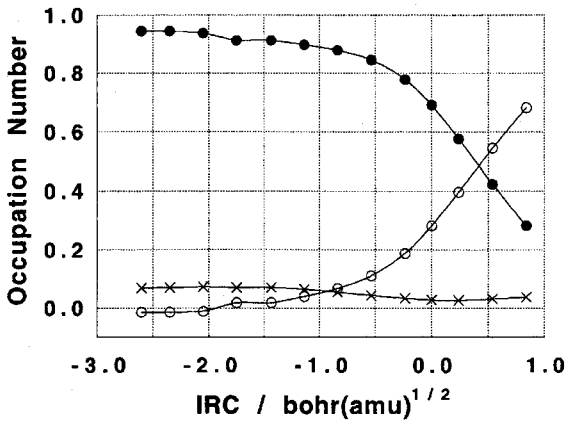

Fig. 8. Changes in the occupation numbers of the total CH bonds (•), total HH bond (○), and the other (doubly ionic) (×) VB structures of H_2CO along the IRC.

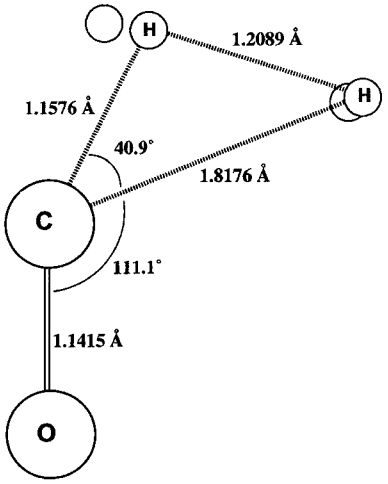

Fig. 9. The structure where the total occupation numbers of the CH bonds and HH bond valence bond structures are equal. The hydrogen atoms not bonded to the carbon atom represent the position at the TS.

$$n_{CH} = n_{\text{Covalent CH}} + n_{\text{Ionic CH}}, \qquad n_{HH} = n_{\text{Covalent HH}} + n_{\text{Ionic HH}}. \tag{16}$$

Fig. 7 shows the changes in the occupation numbers of the covalent CH bonds, ionic CH bonds, covalent HH bond, ionic HH bond, and the other (doubly ionic) structures along IRC. The origin of the horizontal axis corresponds to TS and the left end of each curve to the equilibrium structure. The occupation numbers of CH and HH covalent bond structures change rapidly near TS and the curves cross immediately after TS (0.1 bohr(amu)$^{1/2}$), while the occupation numbers of CH and HH ionic bond structures change slowly.

Fig. 8 shows the changes in the total occupation numbers of the CH and HH bond structures along the IRC. The crossing point is located after TS, 0.42 bohr(amu)$^{1/2}$. The structure at this point is given in Fig. 9. Compared to the TS, the longer and shorter CH bonds have stretched by 0.14 and 0.06 Å, respectively, and the HH bond has become shorter by 0.18 Å. These bond lengths are 1.03, 1.62, and 1.80 times longer than the corresponding equilibrium CH and HH bond distances. That point is the structure where the bonds switch; in other words, the point is the *transition state of chemical bond* between the CH bonds and HH bond.

The results here demonstrate the total occupation number defined in Eq. (16) is a useful concept for studying quantitative description of chemical bonds at TS and along reaction paths.

3.2. Hydrogen exchange reactions H_2+X → H+HX (X=F, Cl, Br, and I)

In the previous subsection, we applied the CASVB method to the unimolecular dissociation reaction $H_2CO \rightarrow H_2 + CO$, and examined how chemical bonds and electronic structures are described along the chemical reaction path. Our focus was on the chemical bond nature in the transition (TS) structure, that is, which bonds are dominant in TS, the dissociating CH bonds or the forming HH bond. The CASVB method shows that CH bonds are dominant in TS, based on the contribution of the VB structure of each bond. This kind of question is not easily answered using the CI picture with canonical molecular orbitals (MOs), and hence this is an example that demonstrates CASVB as a useful tool for analyzing electronic structures and chemical bond during chemical reactions. However, in this reaction the dissociating and forming bonds are both of covalent nature, that is, the bias of the charge is not so large, and thus the description is relatively easy compared to the reaction including ionic bonds.

In the this subsection, we examine a series of reactions including ionic bonds,

$$H_2 + F \rightarrow H + HF, \quad \text{(R1)}$$
$$H_2 + Cl \rightarrow H + HCl, \quad \text{(R2)}$$
$$H_2 + Br \rightarrow H + HBr, \quad \text{(R3)}$$
$$H_2 + I \rightarrow H + HI. \quad \text{(R4)}$$

The reaction for fluorine (R1) is highly exothermic, while the reactions for chlorine (R2), bromine (R3), and iodine (R4) are endothermic. The heats of these reactions are 30.8, −1.2, −16.7, and −32.7 kcal/mol for reactions (R1), (R2), (R3), and (R4), respectively. According to Hammond's postulate, reaction (R1) should have an early TS, and reactions (R2) and (R3) should have late TSs. On the other hand, the electronegativity (in Pauling's definition) for hydrogen, fluorine, chlorine, bromine, and iodine are 2.2, 4.0, 3.2, 3.0, and 2.7, respectively. This suggests that all the reactions (R1)-(R4) might have early TSs, since halogen atoms tend to receive an electron and form the bond with a hydrogen atom at early stage. What the electronic states are during these reactions, and how the CASVB method describes the electronic structure, are our interests in this subsection.

We first determined IRC for each reaction and then obtained the CASVB functions along IRC.

The basis sets used in the reactions including F and Cl are the augmented correlation consistent polarized valence double zeta (aug-cc-pVDZ) sets [16]. In the reactions including Br and I, the relativistic effective core potential (ECP) due to Stevens et al. [17,18] and their associated basis sets were used for Br and I, and the cc-pVDZ set for H. The basis sets of Br and I were augmented by adding a *d* polarization function with an exponent of 0.389 (Br) / 0.266 (I) and *sp* diffuse functions with an exponent 0.03574 (Br) / 0.03007 (I). The diffuse *p* polarization function of the aug-cc-pVDZ set of H was omitted for consis-

tency with the Br and I basis sets.

The active spaces were constructed by distributing three electrons in three orbitals consisting of $H_1(1s)$, $H_2(1s)$, and $X(2p\sigma)$, i.e. CAS(3,3). The dimension of the CAS is eight. According to this CAS, eight linearly independent VB structures,

$$\varphi_{H_A}\varphi_{H_B}(\alpha\beta-\beta\alpha)\cdot\varphi_X\alpha \qquad H_A-H_B\ \dot{X}, \qquad \text{(I)}$$

$$\varphi_{H_B}\varphi_{H_B}\alpha\beta\cdot\varphi_X\alpha \qquad H_A^+\ {}^-H_B\ \dot{X}, \qquad \text{(II)}$$

$$\varphi_{H_A}\varphi_{H_A}\alpha\beta\cdot\varphi_X\alpha \qquad H_A^-\ {}^+H_B\ \dot{X}, \qquad \text{(III)}$$

$$\varphi_{H_A}\alpha\cdot\varphi_{H_B}\varphi_X(\alpha\beta-\beta\alpha) \qquad \dot{H}_A\ H_B-X, \qquad \text{(IV)}$$

$$\varphi_{H_A}\alpha\cdot\varphi_{H_B}\varphi_{H_B}\alpha\beta \qquad \dot{H}_A\ H_B^-\ {}^+X, \qquad \text{(V)}$$

$$\varphi_{H_A}\alpha\cdot\varphi_X\varphi_X\alpha\beta \qquad \dot{H}_A\ H_B^+\ {}^-X, \qquad \text{(VI)}$$

$$\varphi_{H_B}\alpha\cdot\varphi_X\varphi_X\alpha\beta \qquad H_A^+\ \dot{H}_B\ {}^-X, \qquad \text{(VII)}$$

and

$$\varphi_{H_A}\varphi_{H_A}\alpha\beta\cdot\varphi_{H_B}\alpha \qquad H_A^-\ \dot{H}_B\ {}^+X, \qquad \text{(VIII)}$$

were used to construct CASVB functions, where the normalization constants and antisymmetrizers are omitted.

The contributions of the covalent H_AH_B bond, ionic H_AH_B bond, covalent H_BX bond, ionic H_BX bond, and ionic H_AX bond are defined by

$$n_{\text{Covalent }H_AH_B}=n_{\text{I}}, \qquad n_{\text{Ionic }H_AH_B}=n_{\text{II}}+n_{\text{III}}, \qquad (17)$$

$$n_{\text{Covalent }H_BX}=n_{\text{IV}}, \qquad n_{\text{Ionic }H_BX}=n_{\text{V}}+n_{\text{VI}}, \qquad (18)$$

and

$$n_{\text{Ionic }H_AX}=n_{\text{VII}}+n_{\text{VIII}}. \qquad (19)$$

Furthermore, the contributions of the total H_AH_B and H_BX bond structures are defined by the sums of the covalent structure (I)/(IV) and ionic structures (II)/(V) and (III)/(VI),

$$n_{H_AH_B}=n_{\text{Covalent }H_AH_B}+n_{\text{Ionic }H_AH_B}, \qquad n_{H_BX}=n_{\text{Covalent }H_BX}+n_{\text{Ionic }H_BX}. \qquad (20)$$

Table 2
Occupation numbers of the VB structures in the products

		(H+) HF	(H+) HCl	(H+) HBr	(H+) HI
$\dot{H}\ \ H-X$	(IV)	0.538	0.710	0.752	0.786
$\dot{H}\ \ H^{-}\ ^{+}X$	(V)	−0.018	0.041	0.064	0.101
$\dot{H}\ \ H^{+}\ ^{-}X$	(VI)	0.480	0.249	0.184	0.113

Let us first examine the electronic structure at the TS structure of the four reactions as well as those at the reactant and product structures.

The nonorthogonal LMOs were determined in the same manner as in the previous subsection. The atomic orbitals used for the determination are two $1s$ orbitals of the hydrogen atoms and $2p(\sigma)$ orbitals of the halogen atom. All the overlaps between the atomic orbital (AO) and the nonorthogonal LMO are greater than 0.9 (0.9004 at minimum). The molecular orbitals are therefore well localized.

The reactant in all the reactions is the system consisting of a hydrogen molecule and a halogen atom. Since the hydrogen molecule is expressed with VB structures as

$$\Psi_{H_2} = 0.889\left[\varphi_{H_A}\varphi_{H_B}(\alpha\beta-\beta\alpha)/\sqrt{2}\right]+0.111\left[\varphi_{H_A}\varphi_{H_A}\alpha\beta+\varphi_{H_B}\varphi_{H_B}\alpha\beta\right], \qquad (21)$$

Table 3
Occupation numbers of the VB structures at the TS

		H + H + F	H + H + Cl	H + H + Cl	H + H + Cl
$H-H\ \dot{X}$	(I)	0.485	0.328	0.217	0.172
$H^{+}\ ^{-}H\ \dot{X}$	(II)	0.053	0.059	0.043	0.034
$H^{-}\ ^{+}H\ \dot{X}$	(III)	0.017	−0.022	−0.023	−0.019
$\dot{H}\ \ H-X$	(IV)	0.252	0.385	0.514	0.591
$\dot{H}\ \ H^{-}\ ^{+}X$	(V)	−0.005	0.018	0.042	0.073
$\dot{H}\ \ H^{+}\ ^{-}X$	(VI)	0.147	0.155	0.142	0.100
$H^{-}\ \dot{H}\ ^{+}X$	(VII)	0.006	0.013	0.011	0.010
$H^{+}\ \dot{H}\ ^{-}X$	(VIII)	0.045	0.064	0.053	0.039
HH bond		0.555	0.365	0.237	0.187
HX bond		0.394	0.558	0.698	0.764
Others		0.051	0.077	0.064	0.049

the reactant is written as

$$\Psi_{\text{Reactant}} = 0.889[(\text{I})] + 0.111[(\text{II}) + (\text{III})] \tag{22}$$

in all the reactions.

On the other hand, the products are the systems consisting of a hydrogen atom and a hydrogen halide. The VB structures are summarized in Table 2. As mentioned before, the electronegativities of all the halogen atoms are larger than that of the hydrogen atom. In particular, the difference between the electronegativity of F and H atoms, 4.0 and 2.2, respectively, is rather large. Hence, the bond nature of the HF molecule is thought to be ionic. However, the *covalent* nature is found to be dominant in all the hydrogen halide in the CASVB picture, even in the case of HF.

Table 3 shows the VB structure at the TSs of H_2+X → H+HX. Just as for the equilibrium structures, the covalent VB structures are dominant: the structures are well described by the superposition of the HH and HX covalent struc-

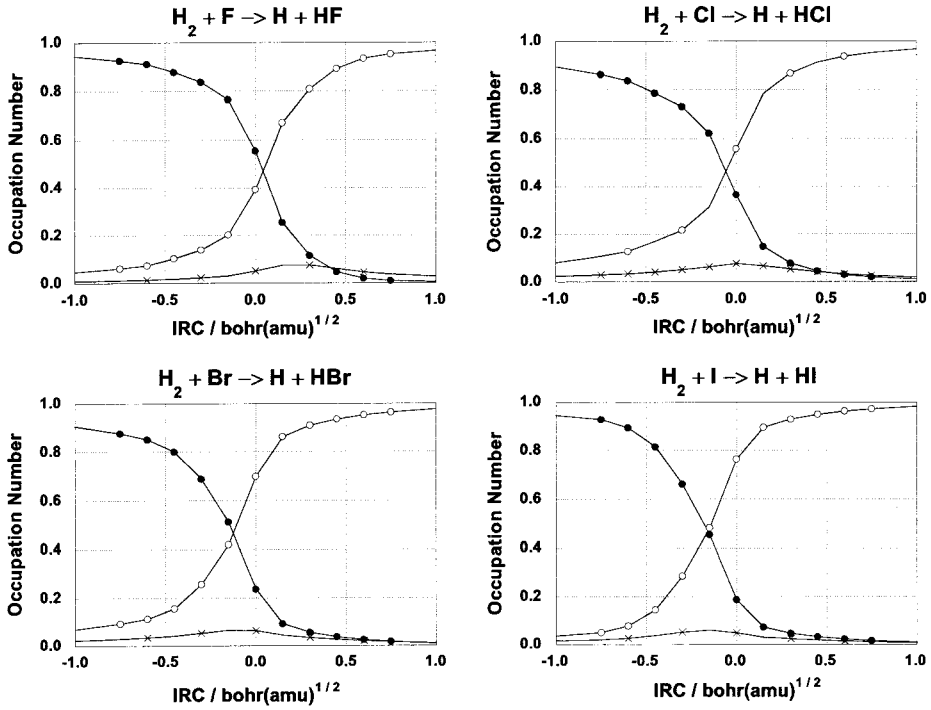

Fig. 10. Changes in the occupation numbers of the total HH bond (•), total HX bond (○), and the other (×) VB structures along IRC. The origin of the horizontal axis corresponds to the TS.

ture with small H^+H and H^+X^- ionic contributions.

Using Eq. (20), these structures are further classified as the HH and HX bonds, as shown in Table 3. For X=F, the contribution of the HH bond (55.5%) is larger than that of the HX bond (39.4%). This relation is reversed for X=Cl, Br, and I. The contribution of the HH bond increases as the halogen atom becomes heavier (55.8 (Cl), 69.8 (Br), and 76.4% (I)). This means that *the TS of chemical bonds* (that is, the point where the occupation numbers of the two chemical bonds are equal) defined in the previous subsection is placed in the reactant side in the X=F case and in the product side for the case of X=Cl, and it shifts more to the product side as the halogen atom becomes heavier.

We now examine the bond nature during the reactions.

Fig. 10 shows the changes in the total occupation number of the HH and HX bond structures along the IRC. Similarly to the previous reaction, the occupation numbers of the HH and HX bond structures change rapidly and the curves cross near the TS. The crossing points are located at 0.07, −0.11, −0.25, and −0.33 bohr(amu)$^{1/2}$ for X=F, Cl, Br, and I, respectively, where a negative sign means the crossing point is located before the TS and a positive sign after the

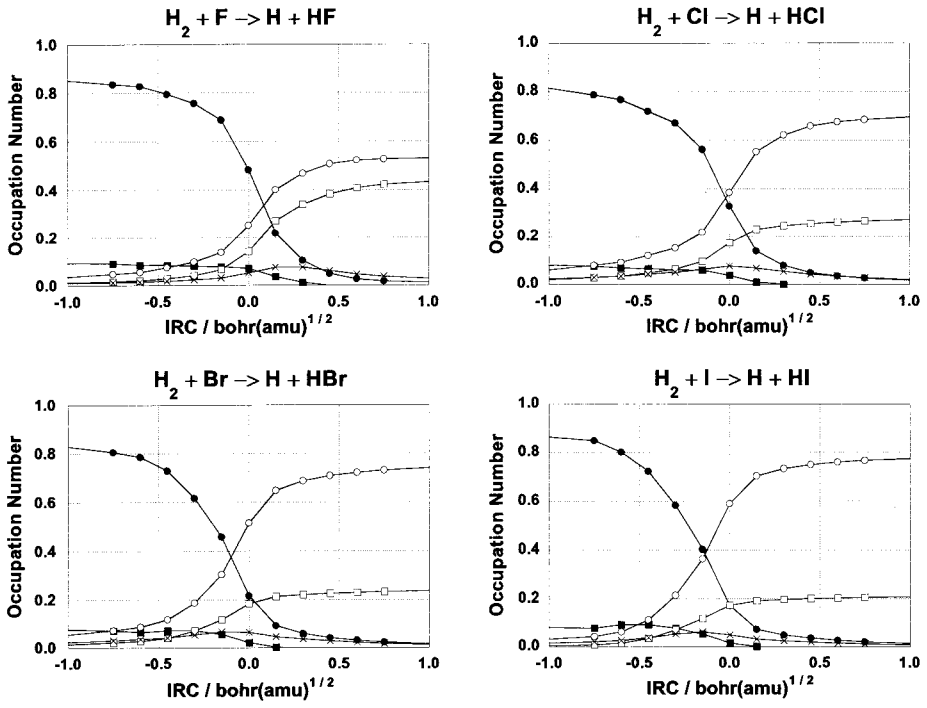

Fig. 11. Changes in the occupation numbers of the covalent HH bond (●), ionic HH bond (■), covalent HX bond (○), ionic HX bond (□), and the other (×) VB structures along the IRC.

TS. We can see the trend that the crossing point shifts from the reactant side to the product side as the halogen atom gets heavier. (We can also consider that the TS shifts from the product side to reactant side if we take the crossing point as the origin.)

The changes in the contents of the HH and HX bonds are plotted in Fig. 11. As expected in these reactions including ionic bonds, the contribution of ionic bond increases as that of the covalent bond increases. This feature contrasts with that in the dissociation reaction of H_2CO, where the ionic bonds do not change so much. However, the crossing point of HH and HX covalent bonds are still close to that of the HH and HX bonds in Fig. 10. Thus, also in these reactions, we can say that the covalent bonds are mainly responsible for determining the crossing points.

To analyze the crossing points, that is, *the TS structures of the HH and HX bonds*, we further examine the geometrical changes of the HH and HX bonds and the dipole moment of the systems.

Fig. 12 presents the difference of the HH and HX bond lengths from the equilibrium lengths along the IRC. It is rather difficult to determine the point

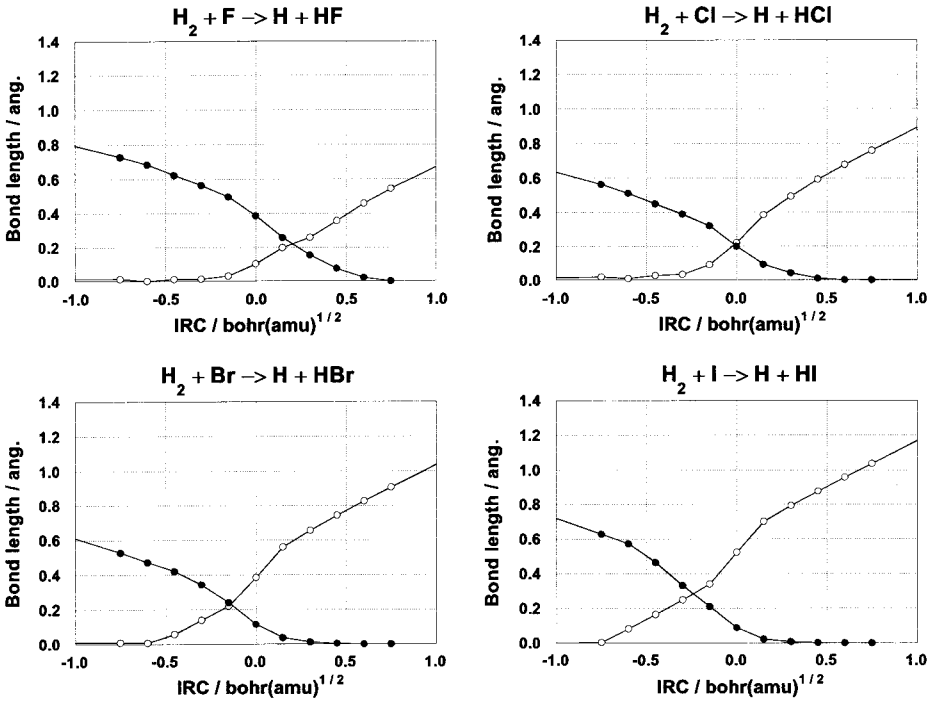

Fig. 12. Differences of the HH (○) and HX (●) bond lengths from the equilibrium lengths along the IRC.

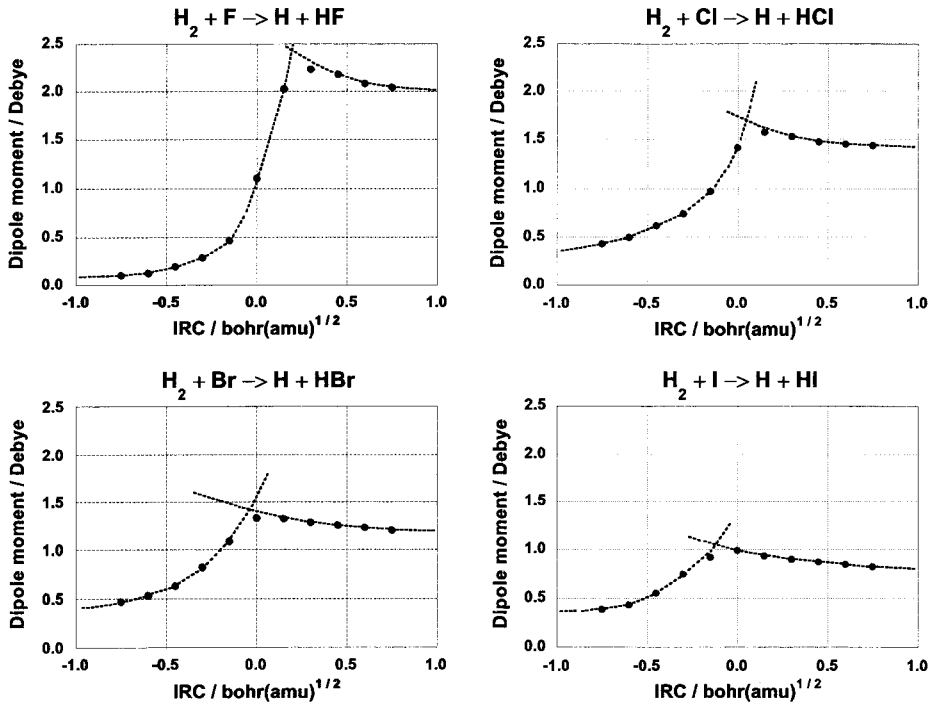

Fig. 13. Changes in dipole moment of the systems along the IRC.

that characterizes the TS. However, for qualitative discussion, the crossing points of the curves are enough to be the characterizing points: they are located at 0.20 (X=F), −0.02 (Cl), −0.14 (Br), and −0.25 bohr(amu)$^{1/2}$ (I). The trend in these positions is similar to the crossing points of the HH and HX bonds. The same can be seen in the changes in dipole moment of the systems plotted in Fig. 13. The curves are drawn so that either dipole moment value for HH+X or H+H$^{+\delta}$X$^{-\delta}$ could be smooth. The crossing points are considered the points where the charge transfer from H to X occurs (in other words, the points where the electronic structure changes drastically). The points are located at 0.19 (X=F), 0.04 (Cl), −0.04 (Br), and −0.13 bohr(amu)$^{1/2}$ (I).

We have now another TS, *the TS of the HH and HX bonds*, besides the real TS. What is the significance of this TS?

If we measure the crossing points in Figs. 12 and 13 from the crossing points of the HH and HX bonds, the values become 0.13 (F), 0.09 (Cl), 0.11 (Br), and 0.08 (I) for geometrical change, and 0.12 (F), 0.15 (Cl), 0.21 (Br), and 0.20 (I) for dipole moment. The ranges of the values are 0.05 for the former numbers and 0.09 for the latter numbers. These are rather small compared to those for the numbers measured from the real TS: 0.45 and 0.32. We may therefore say

that *the TS of chemical bonds* reflects the geometrical and electronic structure information more than the real TS. If we consider Hammond's postulate, probably we should not say that *the TS of chemical bonds* are shifted from the real TS, but instead say that the real TS is shifted from *the TS of chemical bonds* due to the systematic changes in heat of the reaction.

4. CONCLUDING REMARKS

In this article, we investigated the nature of bonds at TS and during the chemical reaction using the CASVB method with nonorthogonal LMOs. The nature of bond dissociation and formation can be viewed quantitatively by the use of the occupation number of the VB structure, which is defined by the weight of the spin-paired function of VB structure. The results in the previous section demonstrate that the occupation number is a useful concept for studying quantitative descriptions of chemical bonds at TS and along reaction paths. This analysis is applicable to reactions involving excited states as well as just the ground state. We believe that the CASVB occupation number analysis is a useful tool for understanding chemical reaction mechanisms.

ACKNOWLEDGMENT

The present research is supported in part by a Grant-in-Aid for Scientific Research on Priority Areas "Molecular Physical Chemistry" from the Ministry of Education, Culture, and Sports, Science and Technology of Japan. One of the authors (HN) acknowledges a Grant-in-Aid for Scientific Research from the Japan Society for the Promotion of Science. The CASSCF and CASVB wave functions were obtained by a modified version of HONDO98 (Ref. 19). The orbital contour maps were plotted using a PLTORB program in GAMESS (Ref. 20).

REFERENCES

[1] K. Hirao, H. Nakano, K. Nakayama, and M. Dupuis, J. Chem. Phys. 105 (1996) 9227.
[2] K. Hirao, H. Nakano, and K. Nakayama, J. Chem. Phys. 107 (1997) 9966.
[3] K. Nakayama, H. Nakano, and K. Hirao, Int. J. Quantum Chem. 66 (1998) 157.
[4] Y. Kawashima, K. Nakayama, H. Nakano, and K. Hirao, Chem. Phys. Lett. 267 (1997) 82.
[5] H. Nakano, K. Nakayama, and K. Hirao, J. Mol. Struct. (Theochem) 461-462 (1999) 55.

[6] K. Ruedenberg, M.W. Schmidt, M.M. Gilbert, and S.T. Elbert, Chem. Phys. 71 (1982) 41.
[7] K. Ruedenberg, M.W. Schmidt, and M.M. Gilbert, Chem. Phys. 71 (1982) 51.
[8] K. Ruedenberg, M.W. Schmidt, M.M. Gilbert, and S.T. Elbert, Chem. Phys. 71 (1982) 65.
[9] J.M. Foster and S.F. Boys, Rev. Mod. Phys. 32 (1960) 300.
[10] T. Thorsteinsson, D.L. Cooper, J. Gerratt, P.B. Karadakov, and M. Raimondi, Theor. Chim. Acta 93 (1996) 343.
[11] T. Thorsteinsson and D.L. Cooper, Theor. Chim. Acta 94 (1996) 233.
[12] T. Thorsteinsson, D.L. Cooper, J. Gerratt, and M. Raimondi, Theor. Chim. Acta 95 (1997) 131.
[13] T. Thorsteinsson, D.L. Cooper, J. Gerratt, and M. Raimondi, in: R. McWeeny, J. Maruani, Y.G. Smeyers, and S. Wilson (Eds.), Quantum Systems in Chemistry and Physics: Trends in Methods and Applications, Kluwer, Dordrecht, 1997.
[14] D.L. Cooper, T. Thorsteinsson, and J. Gerratt, Adv. Quantum Chem. 32 (1998) 51.
[15] T. Thorsteinsson and D.L. Cooper, in: A. Herández-Laguna, J. Maruani, R. McWeeny, and S. Wilson (Eds.), Quantum Systems in Chemistry and Physics. Volume 1: Basic problems and models systems, Kluwer, Dordrecht, 2000.
[16] T.H. Dunning, Jr. J. Chem. Phys. 90 (1989) 1007.
[17] W.J. Stevens, H. Basch, and M. Krauss, J. Chem. Phys. 81 (1984) 6026.
[18] W.J. Stevens, M. Krauss, H. Basch, and P.G. Jasien, Can. J. Chem. 70 (1992) 612.
[19] M. Dupuis, S. Chin, and A. Marquez, in: G.L. Malli (Ed.), Relativistic and Electron Correlation Effects in Molecules and Clusters, NATO ASI Series, Plenum, New York, 1992.
[20] M.W. Schmidt, K.K. Baldridge, J.A. Boatz, S.T. Elbert, M.S. Gordon, J.H. Jensen, S. Koseki, N. Matsunaga, K.A. Nguyen, S. Su, T.L. Windus, M. Dupuis, and J.A. Montgomery, J. Comput. Chem. 14 (1993) 1347.